Research Article Vol. 56, No. 31 / November 1 2017 / Applied Optics 8669

applied optics

Weighted iterative algorithm for beam alignment in scanning beam interference lithography

YING SONG,[1] WEI WANG,[1,2] SHAN JIANG,[1] BAYANHESHIG,[1,*] AND NING ZHANG[1]

[1]National Engineering Research Centre for Diffraction Gratings Manufacturing and Application, Changchun Institute of Optics, Fine Mechanics and Physics, Chinese Academy of Sciences, Changchun Jilin 130033, China
[2]University of Chinese Academy of Sciences, Beijing 100049, China
*Corresponding author: bayin888@sina.com

Received 16 June 2017; revised 16 September 2017; accepted 2 October 2017; posted 3 October 2017 (Doc. ID 298043); published 26 October 2017

To obtain low phase errors and good interference fringe contrast, an automated beam alignment system is used in scanning beam interference lithography. In the original iterative algorithm, if the initial beam deviation is large or the optical parameters are inappropriate, the beam angle (or position) overshoot may exceed the detector's range. To solve this problem, a weighted iterative algorithm is proposed in which the beam angle and position overshoots can be suppressed by adjusting the weighting coefficients. The original iterative algorithm is introduced. The weighted iterative algorithm is then presented and its convergence is analyzed. Simulation and experimental results show that the proposed weighted iterative algorithm can reduce the beam angle and position overshoots at the expense of convergence speed, avoiding the alignment failure caused by exceeding the detector's range. Besides, the original and weighted iterative algorithms can be combined to optimize the iteration. © 2017 Optical Society of America

OCIS codes: (220.1140) Alignment; (220.4830) Systems design; (220.3740) Lithography; (050.2770) Gratings.

https://doi.org/10.1364/AO.56.008669

1. INTRODUCTION

Interference lithography (IL) is an effective, low-cost, flexible technique to fabricate periodic micro/nanostructures [1,2]. Periodic micro/nanostructures have numerous applications in different fields such as spectroscopy, photonic crystals [3], solar cells [4], biotechnology [5], beam formation [6], and high-density data storage [7]. A grating is a kind of typical micro/nanostructure. Particularly, large-area gratings are widely used in chirped-pulse amplification systems and astronomical spectroscopic telescope systems. Although IL is a common method for fabricating gratings, it is difficult and costly to acquire an IL system for producing large-area linear gratings with diameters of several hundred millimeters. The large optics in a conventional IL system are very expensive, and the material defects and dust particles on the lenses may introduce phase nonlinearity [8].

First proposed by Massachusetts Institute of Technology (MIT), scanning beam IL (SBIL) is a method for producing nanometer-accuracy gratings over large areas. In the SBIL system, two small-diameter Gaussian laser beams interfere to produce a low-distortion grating image, and large gratings are fabricated by step-scanning the photoresist-covered substrate underneath the image [9–12]. To obtain good interference fringe contrast and low accumulated phase error, the SBIL system requires tight beam alignment tolerances, where beam angle and position alignment accuracy must reach orders of μrad and μm, respectively. Therefore, an automated beam alignment system was designed. The beam alignment system devised by MIT contains two tip-tilt mirrors for beam angle and position regulation, and a decoupling optical layout to measure the beam angle and position separately. The beam angle and position can be acquired individually from the readings of two position-sensing detectors (PSDs). Based on an iterative algorithm, the desired alignment goal can be achieved by actuating the two tip-tilt mirrors alternately [13,14].

The beam alignment system in SBIL and the laser pointing stabilization system by mechanical mirrors have certain similarities. They are both active systems containing steering mirrors and detectors to steer the objective beam to a target point. Nevertheless, the former does not function in real time, and is operated before the exposure to ensure identical incident angles and good beam position overlaps in the two arms. The latter operates in real time to suppress jitter caused by structural vibrations, acoustic disturbances, and so on [15–17]. Thereupon, beam alignment based on the iterative algorithm satisfies the speed and accuracy requirements of SBIL. Some real-time feedback algorithms applied in the laser pointing stabilization system are not implemented in the beam alignment

system of SBIL [18–21]. The original iterative algorithm developed by MIT is effective [13,14], but the beam angle or position overshoots during the alignment process can be very large. As a result, alignment failures may occur for points that exceed the range of the PSD.

In this paper, the original iterative algorithm is analyzed, and situations that cause large beam angle and position overshoots are identified. An improved weighted iterative algorithm is then proposed, and its convergence property is analyzed mathematically. Additionally, a method that combines the original and weighted iterative algorithms is explored for better performance. The variations in beam angle and position deviation are simulated for comparison, and the experimental results are shown to match the simulations. The weighted iterative algorithm can prevent alignment failures caused by the spot missing the PSD because of beam angle or position overshoots.

2. PRINCIPLE AND ANALYSIS

A. Original Iterative Algorithm and Analysis

The beam alignment system devised by MIT is shown in Fig. 1. M1 and M2 are tip-tilt mirrors. M1 is located farther from the position decoupling plane (PDP). If M1 and M2 have the same tilt angle, M1 brings about a greater change in position at the PDP than M2. Hence, during beam alignment, M1 is used to align the position and M2 is used to align the angle iteratively. Using this optical decoupling system, one PSD (called the position PSD) can only sense the translation at the PDP with a proportion factor of $K_{\text{pos}} = 1 - L_1/f_1$. The beam angle at the angle decoupling plane (ADP) is converted proportionally to the spot location on the other PSD (called the angle PSD). The proportion factor is $K_{\text{angle}} = f_2$. If the two beams are aligned according to the decoupling planes, they have the same position and angle at any point in the optical path after M2. Hence, in this paper, beam "position" and "angle" refer to those at the decoupling planes.

Beam angle and position can be aligned in both X and Y directions. Taking one-dimensional beam alignment for illustration, each iteration contains two steps. In the first step, M1 tilts to zero position deviation. In the following step, zero angle deviation is achieved by actuating M2. Suppose the initial deviations from the desired position and angle are p_0 and a_0, respectively. After the nth iteration, the outputs of position and angle deviation can, respectively, be described in matrix form as

$$\begin{bmatrix} p_{(n,1)} \\ a_{(n,1)} \end{bmatrix} = A \begin{bmatrix} p_{(n-1,2)} \\ a_{(n-1,2)} \end{bmatrix} = A(BA)^{n-1} \begin{bmatrix} p_0 \\ a_0 \end{bmatrix}, \tag{1}$$

$$\begin{bmatrix} p_{(n,2)} \\ a_{(n,2)} \end{bmatrix} = B \begin{bmatrix} p_{(n,1)} \\ a_{(n,1)} \end{bmatrix} = (BA)^{n} \begin{bmatrix} p_0 \\ a_0 \end{bmatrix}, \tag{2}$$

where $p_{(n,1)}$ and $a_{(n,1)}$ are, respectively, the position and angle deviations after the first step of the nth iteration, and $p_{(n,2)}$ and $a_{(n,2)}$ are those after the second step of the nth iteration. In Eqs. (1) and (2), $A = \begin{bmatrix} 0 & 0 \\ -1/D_1 & 1 \end{bmatrix}$ and $B = \begin{bmatrix} 1 & -D_2 \\ 0 & 0 \end{bmatrix}$.

Using matrix operations, we can write

$$A(BA)^{n-1} = \left(\frac{D_2}{D_1}\right)^{n-1} \begin{bmatrix} 0 & 0 \\ -\frac{1}{D_1} & 1 \end{bmatrix}, \tag{3}$$

$$(BA)^{n} = \left(\frac{D_2}{D_1}\right)^{n-1} \begin{bmatrix} \frac{D_2}{D_1} & -D_2 \\ 0 & 0 \end{bmatrix}. \tag{4}$$

For $D_2 < D_1$, the angle and position alignment is convergent and the convergence speed is a function of D_2/D_1 (the smaller the value of D_2/D_1, the faster the convergence [13]).

In the beam alignment process with the original iterative algorithm, the angle overshoot relative to the desired angle is $\max\{a_0, -p_0/D_1 + a_0\}$ and the position overshoot is $\max\{p_0, D_2p_0/D_1 - D_2a_0\}$, which occur in the first iteration. If the initial position deviation p_0 and angle deviation a_0 have opposite signs, the overshoot of the angle is $-p_0/D_1 + a_0$. This may be very large when D_1 is small relative to p_0. If the target location on the angle PSD representing the desired angle is close to the edge of the detector, the spot is likely to exceed the detector's measuring range. This causes the iterative process to fail in the first iteration. A similar situation occurs on the position PSD when D_2/D_1 is close to 1 and D_2 is relatively large.

To solve this problem, three methods have been developed. First, we may choose D_1 to be as large as possible and D_2 as small as possible in the optical design stage. In other words, M2 should be close to the PDP and M1 should be located far away. However, these parameters are sometimes limited by the optical plant size and layout. Second, the initial deviations a_0 and p_0 can be decreased manually before automated beam alignment, but this makes the alignment process inconvenient and complicated. Third, the beam can be aligned with the weighted iterative algorithm described below.

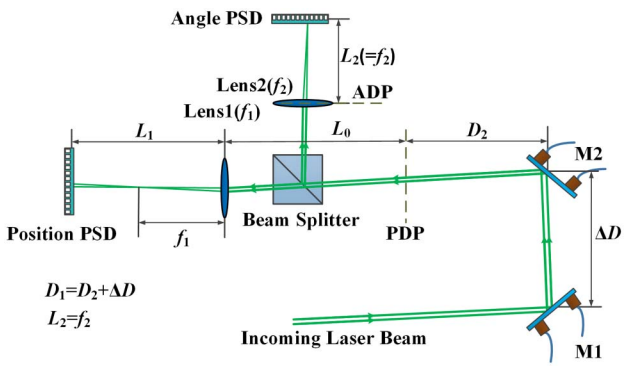

Fig. 1. Optical layout of the automated beam alignment system in SBIL.

B. Weighted Iterative Algorithm

To solve the problem described above automatically, a weighted iterative beam alignment algorithm is proposed. Each iteration again consists of two steps to adjust the position and angle alternately. First, a weight factor k_p ($0 < k_p \le 1$) is applied to the M1 tilting steps. This reduces the position deviation to a certain value (which is nonzero unless $k_p = 1$). Subsequently, another weight factor k_a ($0 < k_a \le 1$) is assigned to the M2 tilting steps to reduce the angle deviation; the angle deviation is also nonzero unless $k_a = 1$.

Suppose the initial position and angle deviations are p_0 and a_0, respectively, before the automated alignment. Take the first

iteration as an example. In the first step, M1 tilts the angle $-k_p p_0/(2D_1)$, resulting in the beam angle changing by $-k_p p_0/D_1$ and the beam position changing by $-k_p p_0$. After the first step, the respective position and angle deviations become

$$\begin{cases} p_{(1,1)} = (1-k_p)p_0 \\ a_{(1,1)} = -\frac{k_p p_0}{D_1} + a_0 \end{cases}. \tag{5}$$

In the next step, M2 tilts the angle $-k_a a_{(1,1)}/2$, resulting in the beam angle changing by $-k_a a_{(1,1)}$ and the position changing by $-k_a a_{(1,1)} D_2$. The output becomes

$$\begin{cases} p_{(1,2)} = p_{(1,1)} - k_a D_2 a_{(1,1)} \\ a_{(1,2)} = (1-k_a)a_{(1,1)} \end{cases}. \tag{6}$$

Similarly, at the beginning of the nth iteration, M1 tilts to reduce the position deviation by $k_p p_{(n-1,2)}$. Then, M2 tilts to reduce the angle deviation by $k_a a_{(n,1)}$. The nth iteration can be described in matrix form as

$$\begin{bmatrix} p_{(n,1)} \\ a_{(n,1)} \end{bmatrix} = A_c \begin{bmatrix} p_{(n-1,2)} \\ a_{(n-1,2)} \end{bmatrix} = A_c (B_c A_c)^{n-1} \begin{bmatrix} p_0 \\ a_0 \end{bmatrix}, \tag{7}$$

$$\begin{bmatrix} p_{(n,2)} \\ a_{(n,2)} \end{bmatrix} = B_c \begin{bmatrix} p_{(n,1)} \\ a_{(n,1)} \end{bmatrix} = (B_c A_c)^n \begin{bmatrix} p_0 \\ a_0 \end{bmatrix}, \tag{8}$$

where

$$A_c = \begin{bmatrix} (1-k_p) & 0 \\ -\frac{k_p}{D_1} & 1 \end{bmatrix} \quad \text{and} \quad B_c = \begin{bmatrix} 1 & -k_a D_2 \\ 0 & 1-k_a \end{bmatrix}.$$

Equations (1) and (7) and Eqs. (2) and (8) have similar formats, and are identical when $k_p = k_a = 1$. This means that the original iterative algorithm can be treated as a special case of the weighted iterative algorithm. In the weighted iterative algorithm, the beam angle and position overshoots can be reduced by adjusting k_p and k_a. For example, if $a_0 < -p_0/D_1 + a_0$, after the first step of the first iteration, the output angle deviation becomes $a_{(1,1)} = -k_p p_0/D_1 + a_0 (k_p < 1)$, which is smaller than the angle overshoot $-p_0/D_1 + a_0$ in the original iterative algorithm.

C. Convergence Property Analysis

The convergence property of the weighted iterative algorithm can be examined based on matrix operations. Let matrix $C = B_c A_c$. For $0 < k_p < 1$ and $0 < k_a < 1$, C can be expressed as $C = T\Lambda T^{-1}$, where $T = [t_1, t_2]$ is formed by eigenvectors t_1 and t_2 of C and $\Lambda = \mathrm{diag}(\lambda_1, \lambda_2)$ contains eigenvalues λ_1 and λ_2 [22]. The eigenvectors and eigenvalues are, respectively,

$$t_1 = \begin{bmatrix} -(M+U)/(2k_p(k_a-1)) \\ 1 \end{bmatrix}, \quad t_2 = \begin{bmatrix} (M-U)/(2k_p(k_a-1)) \\ 1 \end{bmatrix}, \tag{9}$$

$$\lambda_1 = (-M+N)/2D_1, \qquad \lambda_2 = (M+N)/2D_1, \tag{10}$$

where

$$M = [D_1^2(k_p-k_a)^2 + 2D_1 D_2 k_p k_a (2-k_p-k_a) + D_2^2 k_p^2 k_a^2]^{1/2},$$

$$U = D_1(k_p-k_a) - D_2 k_p k_a, \text{ and } N = D_1(2-k_p-k_a) + D_2 k_p k_a.$$

When D_1, D_2, and k_a $(0 < k_a < 1)$ are invariant, the partial derivatives of λ_1 and λ_2 with respect to k_p can be evaluated numerically with Matlab. The results show that both derivatives are negative. The same method shows that the partial derivatives of λ_1 and λ_2 with respect to k_a are also negative.

Thus, in the case of $0 < k_p, k_a < 1$,

$$\lambda_1(1,1) < \lambda_1(k_p, k_a) < \lambda_1(0,0), \lambda_2(1,1) < \lambda_2(k_p, k_a) < \lambda_2(0,0). \tag{11}$$

Calculating the values in Eq. (11), we find that $0 < \lambda_1 < 1$, $D_2/D_1 < \lambda_2 < 1$. Hence,

$$\lim_{n\to\infty} \lambda_1^n = 0, \quad \lim_{n\to\infty} \lambda_2^n = 0. \tag{12}$$

For $C = T\Lambda T^{-1}$, where all elements of T and T^{-1} are finite, the nth power of C as $n \to \infty$ is

$$\lim_{n\to\infty} C^n = \lim_{n\to\infty} T \begin{bmatrix} \lambda_1^n & 0 \\ 0 & \lambda_2^n \end{bmatrix} T^{-1} = 0. \tag{13}$$

The above analysis shows that the alignment process is convergent for $0 < k_p, k_a < 1$. Moreover, for $\lambda_1(1,1) < \lambda_1(k_p, k_a)$ and $\lambda_2(1,1) < \lambda_2(k_p, k_a)$, the convergence speed of the weighted iterative algorithm is slower than that of the original iterative algorithm when $k_p \neq 1$, $k_a \neq 1$. Thus, the reduced overshoot using the weight parameter k_a or k_p is gained at the expense of some alignment convergence speed.

If k_p and k_a are selected arbitrarily, angle or position overshoots may appear in the second iteration and the convergence speed may become very slow. The value of k_p is more significant for angle overshoot, whereas the value of k_a controls the position overshoot. Therefore, it is recommended that the key parameter between k_a and k_p be minimized to reduce the overshoot whereas the other parameter is held constant at 1.

D. Combining the Original Iterative Algorithm with the Weighted Iterative Algorithm

For angle and position overshoots that appear at the beginning of the iteration, the weighted iterative algorithm should be used initially. When the local extremum of angle or position deviation is less than a certain threshold, the original iterative algorithm should be adopted in the subsequent iteration. This ensures that the overshoot is the same as that using the weighted iterative algorithm in the whole alignment process; however, the convergence speed can be improved significantly.

3. SIMULATION

The position and angle changes given by the alignment process are estimated with Matlab. The optical parameters for simulation are $f_1 = 500$ mm, $L_1 = 785$ mm, $f_2 = 400$ mm, $D_1 = 250$ mm, and $D_2 = 100$ mm. To test the effectiveness of the weighted iterative algorithm, D_1 and D_2 are deliberately set to suboptimal values. We find that $K_{\mathrm{pos}} = -0.57$ and $K_{\mathrm{angle}} = 0.4$ μm/μrad. For the initial deviation, let $p_0 = 1$ mm, $a_0 = -500$ μrad, and the alignment tolerances

are set to 30 μm (position) and 30 μrad (angle). We consider the beam alignment in X direction for illustration.

Figure 2 shows the changes in position and angle deviations in the beam alignment process using the original iterative algorithm. The alignment is convergent and the alignment tolerances in position and angle are simultaneously satisfied when the number of iterations $n \geq 7$. However, the angle overshoot reaches −4500 μrad because p_0 and a_0 have opposite signs and D_1 is small relative to p_0, as discussed in Section 2.A. The angle overshoot causes the spot position at the angle PSD to change by $K_{\text{angle}} \times (-4500\ \mu\text{rad}) = -1.8$ mm. Generally, the effective measuring size of the PSDs is several millimeters, so the spot in the angle PSD may easily exceed the range of the detector if the desired angle spot is close to the edge.

Using the weighted iterative algorithm for alignment, we set the weight parameter $k_p = 0.5$ to reduce the angle overshoot, as this system is more sensitive to angle changes. We set $k_a = 1$ and keep the optical parameters the same as those for the above simulation. As shown in Fig. 3, the alignment again converges and the angle overshoot is reduced to −2500 μrad. Correspondingly, the spot position at the angle PSD changes by 1 mm, which is nearly half that in the original iterative algorithm. Nevertheless, the convergence speed is slower, with $n \geq 13$ required to satisfy the alignment tolerances.

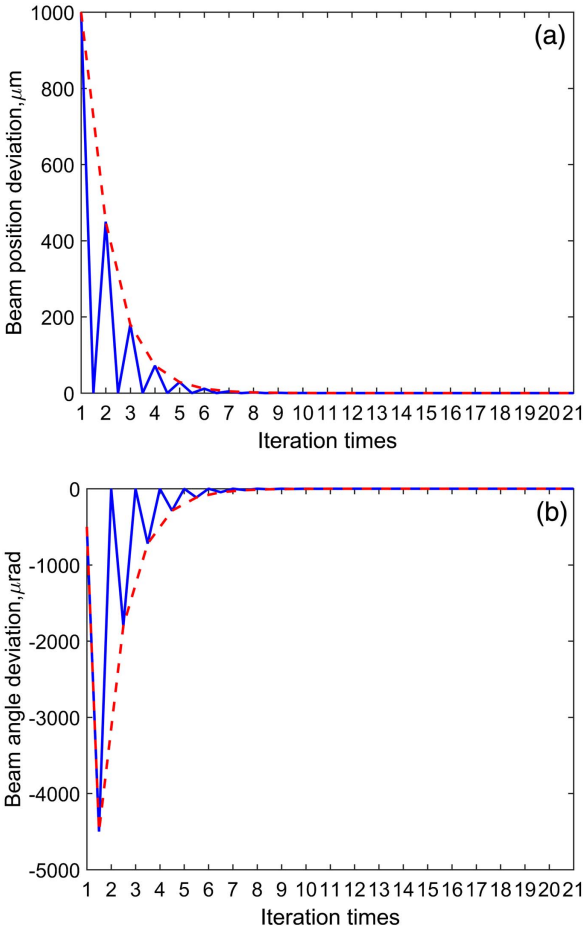

Fig. 2. Beam position and angle deviation changes in the beam alignment process with the original iterative algorithm. Panels (a) and (b) show the beam position and angle deviations, respectively.

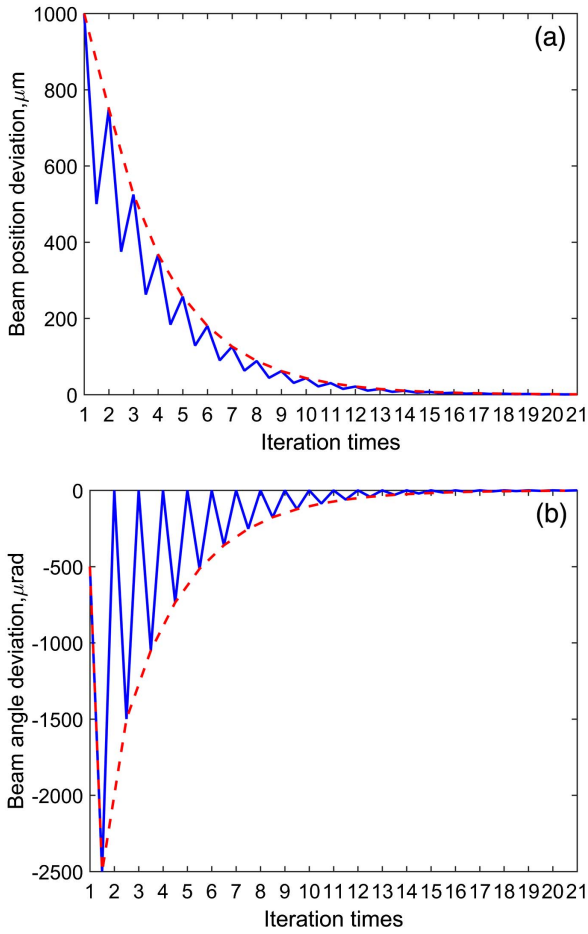

Fig. 3. Beam position and angle deviation changes in the beam alignment process with the weighted iterative algorithm. Panels (a) and (b) show the beam position and angle deviations, respectively.

With $k_a = 1$ and the same optical parameters, the angle overshoot and convergence speed change according to k_p—the smaller the value of k_p, the smaller the angle overshoot and the slower the convergence speed. For example, if $k_p = 0.1$, at least 57 iterations are needed for convergence.

We now combine the original iterative algorithm with the weighted iterative algorithm. Assume that the angle deviation threshold ε_a for switching between the two algorithms is 1250 μrad. If the local extremum of angle deviation is above ε_a, we set $k_p = 0.5$ and $k_a = 1$; otherwise, $k_p = k_a = 1$. As shown in Fig. 4, the maximum angle overshoot is again 2500 μrad. After the fourth iteration, the original iterative algorithm is adopted so the angle deviation converges quickly. Convergence is achieved when $n \geq 9$, which is larger than the value of 7 with the original iterative algorithm, but smaller than the 13 iterations required by the weighted algorithm. The weight parameter k_a can regulate the position overshoot and convergence speed in a similar manner.

4. EXPERIMENTS AND RESULTS

The experimental optical layout is shown in Fig. 5, where BS1–BS3 are beam splitters and M3–M5 are planar mirrors.

The beam from the laser source is split into a reference beam and a regulating beam. Before the beam alignment, the regulating beam is blocked. The reference beam passes through M3, M4, and BS2 before entering the decoupling topology shown in Fig. 1. The spot locations at the position PSD and angle PSD are input into a computer. A Labview-based control program accomplishes the calculation, data recording, and the iterative algorithms. According to the magnification factor of the decoupling topology, the spot locations are converted to beam position and angle, which are recorded and treated as the alignment targets. The reference beam is then blocked and the regulating beam is released. The beam alignment begins. The regulating beam passes through M1, M2, and BS2, and then enters the same decoupling topology. During beam alignment, only regulating beam spots exist on the PSDs. The PSDs provide position and angle information of the regulating beam. The control program calculates the position and angle deviations by subtracting the recorded target values from the measured values of the regulating beam. With the iterative algorithm, the regulating beam is aligned step by step to the target values by tilting M1 and M2.

A 4.7 mW, single-mode laser diode module (CPS532, Thorlabs) operating at a center wavelength of 531.9 nm is used as the light source. The laser source emits a circular beam with a diameter of 3.5 mm. The optical parameters are $f_1 = 500$ mm, $L_1 = 785$ mm, $f_2 = 400$ mm, $D_1 = 1345$ mm, and $D_2 = 616$ mm. D_1 and D_2 are designed for practical applications, unlike in the simulations. The magnification factors of the decoupling topology are $K_{pos} = -0.57$ and $K_{angle} = 0.4$ μm/μrad. The position PSD is an OPB-U-9H and the angle PSD is an OPB-U-4H, both from Newport. M1 and M2 are both 8816-6 (Newport). Each tip-tilt mirror is driven

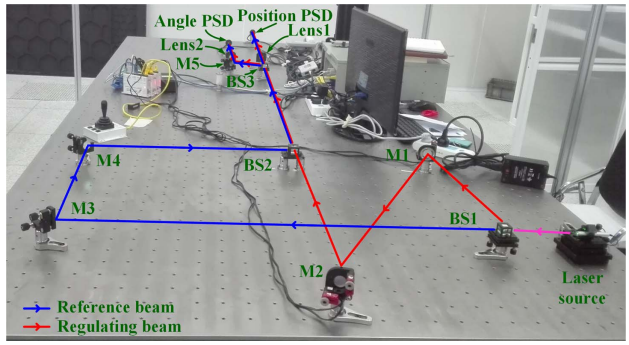

Fig. 5. Photo of the experimental optical layout.

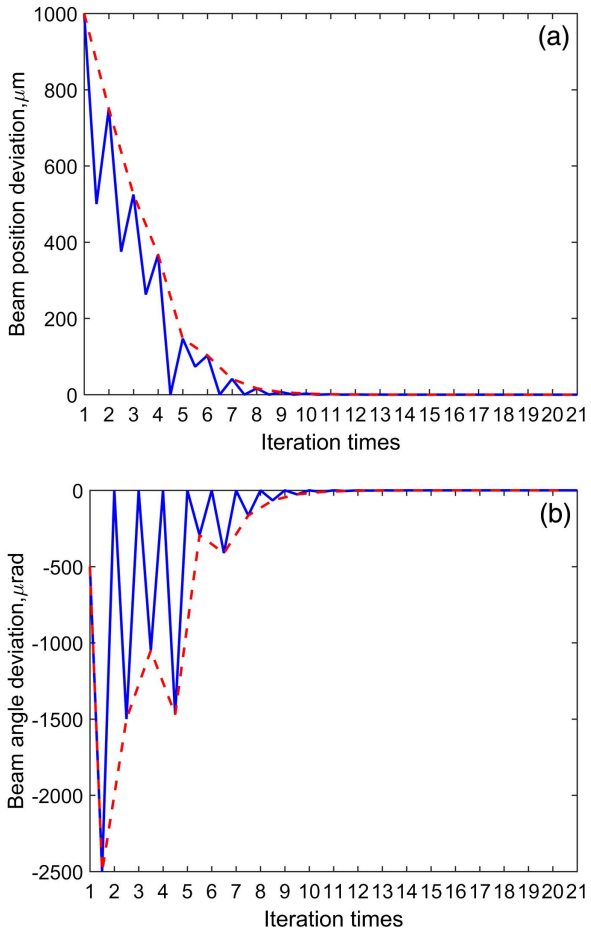

Fig. 4. Beam position and angle deviation changes in the beam alignment process by combining the two algorithms. Panels (a) and (b) show the beam position and angle deviations, respectively.

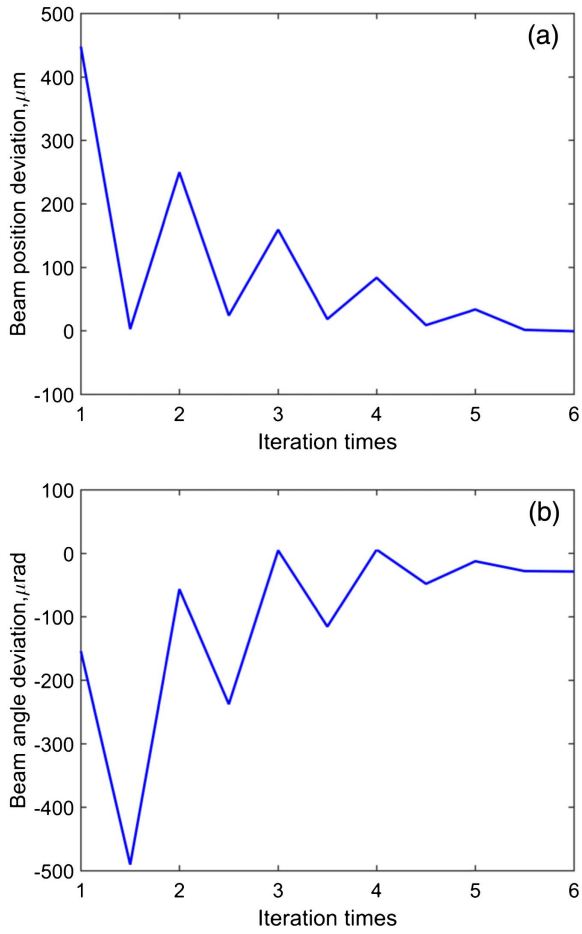

Fig. 6. Experimental results of beam alignment with the original iterative algorithm. Panels (a) and (b) show the beam position deviation and beam angle deviation, respectively.

by two picomotors, each of which is a screw turned by a piezoelectric actuator.

In the experiment, the regulating beam is aligned with the different iterative algorithms in X direction, whereas the reference beam path remains invariant. Thus, the beam alignment targets are theoretically constant. Nevertheless, they may vary slightly because of environmental changes, and so alignment targets are acquired before every alignment. In addition, to ensure similar initial conditions, p_0 and a_0 are adjusted to similar values by rotating the picomotors manually. We set the position and angle alignment tolerances to 30 μm and 30 μrad, respectively. Figures 6–8 show the changes in position and angle deviations in the beam alignment experiment. The position and angle of the regulating beam are measured by the PSDs in each iterative step. The data points in the figures are acquired by subtracting the target values from the measured value of the regulating beam.

As shown in Fig. 6(a) and 6(b), the beam is aligned with the original iterative algorithm ($k_p = k_a = 1$). The initial deviations are $a_0 = -154.1$ μrad and $p_0 = 447.7$ μm. The measured value of angle overshoot is −490.3 μrad, which agrees with theoretical value of $-p_0/D_1 + a_0 = -486.9$ μrad. The local minimum values are nonzero because of the nonlinearity of the picomotors, which is caused by the piezoelectric actuator and the mechanical parts. Alignment is accomplished after five iterations.

Figure 7(a) and 7(b) shows the results of beam alignment with the weighted iterative algorithm. The initial deviations are $a_0 = -148.5$ μrad and $p_0 = 468.2$ μm. The weight parameters are $k_p = 0.5$ and $k_a = 1$. The measured value of angle overshoot is −309.1 μrad, which is lower than that using the original algorithm. The alignment is convergent, but the convergence is slower (requiring $n \geq 10$).

Figure 8(a) and 8(b) shows the beam alignment results obtained by combining the original iterative algorithm with the weighted iterative algorithm. The switching angle deviation threshold is set to $\varepsilon_a = 200$ μrad. Initially, the weighted iterative algorithm is used with $k_p = 0.5$ and $k_a = 1$. Once the local extremum of angle deviation $|a_{(n,1)}| \leq \varepsilon_a$, the weighted parameters change to $k_p = k_a = 1$. The initial deviations are $a_0 = -149.1$ μrad and $p_0 = 443$ μm. The measured angle overshoot is −316.6 μrad, and $n \geq 7$ to satisfy the alignment accuracy requirements. The angle overshoot is close to that in Fig. 7(b), but the convergence is faster.

Although the parameters in the experiment are different from those in the simulation, the beam position and angle

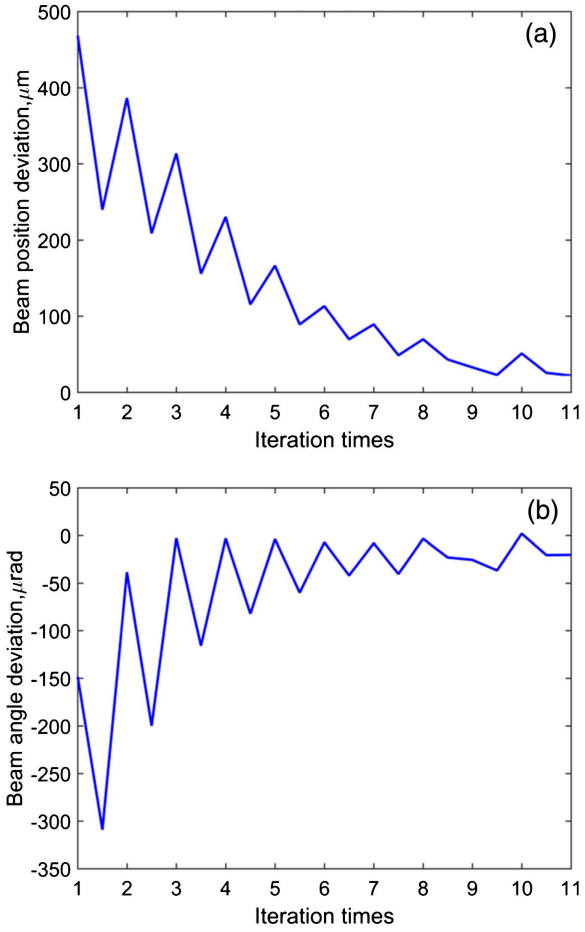

Fig. 7. Experimental results of beam alignment with the weighted iterative algorithm ($k_p = 0.5$, $k_a = 1$). Panels (a) and (b) show the beam position deviation and beam angle deviation, respectively.

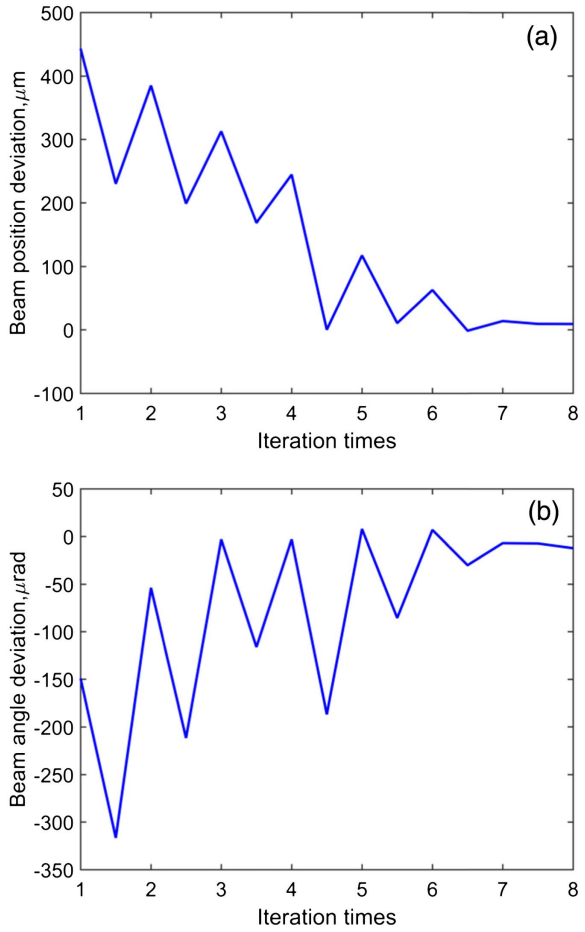

Fig. 8. Experimental results of beam alignment with the combined algorithm. Panels (a) and (b) show the beam position deviation and beam angle deviation, respectively.

deviations show the same trends. The experimental results thus agree with the simulation.

5. CONCLUSION

We have demonstrated a new weighted iterative algorithm for beam alignment in SBIL. The algorithm was demonstrated and its convergence property was analyzed mathematically. The angle and position deviation changes during the alignment process were simulated to compare the weighted iterative algorithm and the original iterative algorithm. An experimental optical layout was designed, and the beam was aligned by the different iterative algorithms. The experimental results agreed with those in the simulation. With the weighted iterative algorithm, regulating the weighting parameters k_p and k_a can reduce the angle and position overshoots, but the convergence is relatively slow. As a result, alignment failures caused by the measuring spot exceeding the detector's range can be avoided at the cost of convergence speed. Moreover, combining the original iterative algorithm with the weighted iterative algorithm, the overshoots are the same as those using the weighted iterative algorithm for the whole beam alignment process; however, the convergence speed is closer to that of the original algorithm. This combined algorithm is more suitable for practical applications.

Funding. National Natural Science Foundation of China (NSFC) (61227901).

REFERENCES

1. C. H. Liu, M. H. Hong, M. C. Lum, H. Flotow, F. Ghadessy, and J. B. Zhang, "Large-area micro/nanostructures fabrication in quartz by laser interference lithography and dry etching," Appl. Phys. A **101**, 237–241 (2010).
2. L. Wang, Z. H. Lü, X. F. Lin, Q. D. Chen, B. B. Xu, and H. B. Sun, "Rapid fabrication of large-area periodic structures by multiple exposure of two-beam interference," J. Lightwave Technol. **31**, 276–281 (2013).
3. J. J. Zhang, Z. B. Wang, X. Di, L. Zhao, and D. P. Wang, "Effects of azimuthal angles on laser interference lithography," Appl. Opt. **53**, 6294–6301 (2014).
4. I. B. Divliansky, A. Shishido, I. C. Khoo, T. S. Mayer, D. Pena, S. Nishimura, C. D. Keating, and T. E. Mallouk, "Fabrication of two-dimensional photonic crystals using interference lithography and electrodeposition of CdSe," Appl. Phys. Lett. **79**, 3392–3394 (2001).
5. M. Malinauskas, P. Danilevičius, E. Balčiūnas, S. Rekštytė, E. Stankevičius, D. Baltriukienė, V. Bukelskienė, G. Račiukaitis, and R. Gadonas, "Application of nonlinear laser nano/microlithography fabrication from nanophotonic to biomedical components," Proc. SPIE **8204**, 820407 (2011).
6. E. Stankevičius, M. Garliauskas, M. Gedvilas, and G. Račiukaitis, "Bessel-like beam array formation by periodical arrangement of the polymeric round-tip microstructures," Opt. Express **23**, 28557–28566 (2015).
7. R. Murillo, H. A. van Wolferen, L. Abelmann, and J. Lodder, "Fabrication of patterned magnetic nanodots by laser interference lithography," Microelectron. Eng. **78**–79, 260–265 (2005).
8. L. Shi, L. J. Zeng, and L. F. Li, "Fabrication of optical mosaic gratings with phase and attitude adjustments employing latent fringes and red-wavelength dual-beam interferometer," Opt. Express **17**, 21530–21543 (2009).
9. P. T. Konkola, *Design and Analysis of a Scanning Beam Interference Lithography System for Patterning Gratings with Nanometer-Level Distortions* (Massachusetts Institute of Technology, 2003).
10. J. Montoya, *Toward Nano-Accuracy in Scanning Beam Interference Lithography* (Massachusetts Institute of Technology, 2006).
11. C. G. Chen, P. T. Konkola, R. K. Heilmann, G. S. Pati, and M. L. Schattenburg, "Image metrology and system controls for scanning beam interference lithography," J. Vac. Sci. Technol. B. **19**, 2335–2341 (2001).
12. C. G. Chen, P. T. Konkola, R. K. Heilmann, C. Joo, and M. L. Schattenburg, "Nanometer-accurate grating fabrication with scanning beam interference lithography," Proc. SPIE **4936**, 126–134 (2002).
13. C. G. Chen, *Beam Alignment and Image Metrology for Scanning Beam Interference Lithography: Fabricating Gratings with Nanometer Phase Accuracy* (Massachusetts Institute of Technology, 2003).
14. P. T. Konkola, C. G. Chen, R. K. Heilmann, and M. L. Schattenburg, "Beam steering system and spatial filtering applied to interference lithography," J. Vac. Sci. Technol. B. **18**, 3282–3286 (2000).
15. V. A. Skormin and M. A. Tascillo, "Jitter rejection technique in a satellite-based laser communication system," Opt. Eng. **32**, 2764–2769 (1993).
16. M. A. McEver and R. L. Clark, "Active jitter suppression of optical structures," Proc. SPIE **4327**, 591–599 (2001).
17. L. Kral, "Automatic beam alignment system for pulsed infrared laser," Rev. Sci. Instrum. **80**, 013102 (2009).
18. R. Singh, K. Patel, J. Govindarajan, and A. Kumar, "Fuzzy logic based feedback control system for laser beam pointing stabilization," Appl. Opt. **49**, 5143–5147 (2010).
19. F. Breitling, R. S. Weigel, M. C. Downer, and T. Tajima, "Laser pointing stabilization and control in the submicroradian regime with neural networks," Rev. Sci. Instrum. **72**, 1339–1342 (2001).
20. T. Kanai, A. Suda, S. Bohman, M. Kaku, S. Yamaguchi, and K. Midorikawa, "Pointing stabilization of a high-repetition-rate high-power femtosecond laser for intense few-cycle pulse generation," Appl. Phys. Lett. **92**, 061106 (2008).
21. A. Stalmashonak, N. I. Zhavoronkov, H. I. Volker, S. Vetrov, and K. Schmid, "Spatial control of femtosecond laser system output with submicroradian accuracy," Appl. Opt. **45**, 1271–1274 (2006).
22. S. J. Leon, *Linear Algebra* (China Machine, 2011).

144.36.173.4 {ts '2018-08-01 18:01:01'}